

Destruction and survival of polycyclic aromatic hydrocarbons in active galaxies

G. Mark Voit

California Institute of Technology, Theoretical Astrophysics, Mail Code 130-33, Pasadena, CA 91125, USA

Accepted 1992 July 10. Received 1992 July 6; in original form 1991 August 12

ABSTRACT

Infrared spectra of dusty galactic environments often contain emission features attributed to polycyclic aromatic hydrocarbons or PAHs, which can be considered to be very small grains or very large molecules. Although IR spectra of starburst galaxies almost always show these emission features, similar spectra of active galaxies are usually featureless. Even in those active galaxies that do exhibit PAH emission, the PAHs still appear to be eradicated from the nuclear region. This dichotomy suggests that PAHs are destroyed by the intense hard radiation field from an AGN. Laboratory experiments show that certain PAHs are, in fact, so effectively destroyed by individual EUV and X-ray photons that they cannot survive even at kiloparsec distances from active nuclei. Regions within active galaxies that *do* show PAH emission must therefore be shielded from the central X-ray source by a substantial column density of X-ray absorbing gas. Two-dimensional maps of 3.3- μm emission from active galaxies might be useful in determining the anisotropy of ionizing radiation emerging from the central source along directions within the plane of the host galaxy.

Key words: molecular processes – dust, extinction – galaxies: active – galaxies: interstellar matter – galaxies: starburst – infrared: galaxies.

1 INTRODUCTION

Almost a decade ago in a series of pioneering papers, Aitken, Roche and collaborators established that the mid-IR spectra of active galaxies differ markedly from those of starburst galaxies: starburst galaxies show prominent 8.7- and 11.3- μm emission features, while the spectra of active galaxies are usually featureless. Roche et al. (1991) summarize these observations and provide the appropriate references. Since this spectral difference is so distinct, Roche et al. (1991) argue that, if nuclear starbursts develop into active galactic nuclei (AGNs), the transition must occur quite rapidly. Certainly, understanding the relationships between starburst and AGN phenomena will entail understanding this dissimilarity in their mid-IR behaviour.

During the last few years, the identification of the 3.3-, 6.2-, 7.7-, 8.7- and 11.3- μm emission features with various bending and stretching modes of polycyclic aromatic hydrocarbons (PAHs) (Leger & Puget 1984; Allamandola, Tielens & Barker 1985) has become progressively more secure (Puget & Léger 1989; Allamandola, Tielens & Barker 1989), but problems still remain (see e.g. Donn, Allen & Khanna 1989). According to the ‘PAH hypothesis’, transient heating by individual near-UV (< 13.6 eV) photons excites the mid-IR emission, implying that interstellar PAH mole-

cules must contain ≤ 100 carbon atoms (Sellgren 1984). The colour temperature derived from the 3.3- to 11.3- μm band intensity ratio further constrains the PAH size to be roughly 20–40 carbon atoms (Allamandola et al. 1989), although Puget & Léger (1989) obtain a somewhat higher estimate of ~ 90 carbon atoms per PAH.

Recognizing that the hard radiation field within an active galaxy is likely to be especially hostile to PAHs, Aitken & Roche (1985) hypothesized that the absence of PAH emission was due to the destruction of these molecules by EUV photons. Voit (1991), in a study of grain heating by X-rays, showed that grains ≤ 10 Å in radius are indeed destroyed by hard photons, but since this study used solid-state properties to model very small grains, it did not directly address the fate of molecular particles such as PAHs. Aggregates of ≤ 100 atoms are unlikely to behave like solid-state systems, so a complete study of PAH destruction needs to account for the molecular nature of these particles.

This paper examines how the high-energy photons from an AGN affect PAHs in the surrounding galaxy, and explores how PAH emission can be used as a diagnostic of the radiation field within active galaxies. The following section (2) argues that PAH photodestruction, rather than some other effect, is responsible for the absence of the mid-IR emission features, and Section 3 describes how UV and X-ray

photons interact with and destroy PAHs. In Section 4 we evaluate whether C and H accretion can compensate for photodestruction, and in Section 5, we discuss how X-ray shielding allows PAHs to survive in at least a few active galaxies. Section 6 summarizes our results. Although the paper presumes that the PAH hypothesis is correct, its qualitative conclusions apply to any transiently heated hydrocarbon species in the ISM; thermally isolated clusters of hydrocarbons that heat to ~ 1000 K under near-UV irradiation ought to disintegrate under X-ray irradiation.

2 THE ABSENCE OF PAH EMISSION IN ACTIVE GALAXIES

The mid-IR survey of Aitken & Roche measured the emission spectra emerging from within radii of 2–2.5 arcsec around the nuclei of various galaxies, and detected PAH emission in only ~ 10 per cent of active galaxies. In contrast, the same survey detected PAH emission in ≥ 90 per cent of starburst galaxies. Even when PAH emission is present in an active galaxy, the features are often not associated with the nucleus but rather with an extended, probably starburst, region (Cutri et al. 1984; Désert & Dennefeld 1988). In apertures larger than the 5 arcsec used by Aitken & Roche, 3.3- μm features are occasionally detected in galaxies with featureless, small-aperture mid-IR spectra (Moorwood 1986), indicating that perhaps the AGN creates a PAH ‘zone of avoidance’ within the central kiloparsec (Désert & Dennefeld 1988). In this section we will discuss how PAH emission is distributed in our own Galaxy and argue that photo-destruction eliminates PAHs near active nuclei.

2.1 Galactic PAH emission

PAH emission at 3.3- μm is ubiquitous in the interstellar medium (ISM) of our own Galaxy (Giard et al. 1988) but is most pronounced in well-illuminated regions such as reflection nebulae and the neighbourhoods of H II regions. Transient excitation of PAHs by the interstellar UV field accounts for this emission, which brightens as the ambient radiation field intensifies, and the relative strengths of the PAH features depend primarily on the average energy per absorbed photon. Thus a standard PAH emission signature traces UV-heated dusty gas throughout our ISM.

When examined in more detail, PAH emission appears to vanish within H II regions themselves (Sellgren 1981) while remaining bright just across the ionization front. Either PAHs cannot survive the intensity of the radiation field near O and B stars, or they cannot withstand irradiation by EUV photons. Two-photon heating events, in which two near-UV photons are absorbed in less than a PAH cooling time, can potentially evaporate smaller PAHs (< 25 C atoms) near O and B stars, but do not similarly affect larger ones (Omont 1986). Ionizing EUV photons, which do not cross the ionization front, disturb the larger species more dramatically, and are therefore more likely to be the primary agent of PAH destruction in H II regions (Leach 1987).

2.2 PAH destruction by energetic photons

Aitken & Roche (1985), when confronted with the distinct mid-IR dichotomy between starburst and Seyfert nuclei,

proposed that the EUV photon flux in Seyfert galaxies rids the surrounding interstellar media of their PAHs, noting that PAHs within a few hundred parsecs of an average Seyfert nucleus would absorb 20–40 eV photons on a short time-scale. This attractive proposal has two drawbacks: (i) EUV photons cannot penetrate deeply into the neutral media which radiate the majority of the galactic PAH emission, and (ii) intrinsic starburst and Seyfert luminosities in the 1–2 Ryd range are similar, producing equivalent radiative energy densities in the ≥ 300 -kpc circumnuclear regions, yet starbursts still manage to emit strong PAH features. These problems can be resolved if we hypothesize that X-ray photons, rather than EUV photons, eliminate the PAHs near AGNs.

Photon penetration depths increase with photon energy, so destroying PAHs at a column depth of $\sim 10^{20-21}$ cm^{-2} , where the near-UV photons are converted into PAH emission, requires photons of ≥ 200 eV. At these photon energies, the fluxes intrinsic to starburst and Seyfert galaxies differ distinctly: hot-star luminosities drop exponentially into the X-ray regime, whereas Seyfert galaxies remain powerful. Even though PAHs are more transparent to soft X-rays than to EUV radiation, we will show below (Section 4) that X-ray destruction is more than rapid enough to account for the eradication of PAHs from Seyfert nuclei.

2.3 Other explanations for the absence of PAH emission

Before we discuss more fully how EUV and X-ray photons destroy PAHs, let us first consider whether some other mechanism might be responsible for the lack of PAH emission in AGNs. In subsequent sections, we will assume that PAH-free, radiatively heated dust clouds emit much of the IR flux from AGNs, but alternative possibilities are (i) non-thermal IR emission swamps the thermal emission from typical PAH-bearing dust clouds, or (ii) PAHs exist within AGN-irradiated dust clouds, but optical depth effects conspire to suppress their emission features. We discuss and dismiss both of these alternatives in the following paragraphs.

2.3.1 Does no PAH emission imply no thermal emission?

An AGN whose IR continuum emission is overwhelmingly non-thermal will not exhibit significant PAH features, but even a modest amount of dust obscuration will dilute the non-thermal continuum with appreciable thermal emission (e.g. Carleton et al. 1987). If PAHs are not selectively destroyed, mid-IR emission features will accompany the thermal spectrum. One would then expect the presence of PAH features to correlate with the relative importance of the thermal continuum. In many, if not all active galaxies, however, the thermal contribution seems to dominate the non-thermal especially in Seyfert 2 galaxies (Carleton et al. 1987; Sanders et al. 1989), yet PAH features are rarely seen. In particular, PAH features are absent from the nuclear spectra of NGC 1068 (Roche et al. 1984) and Mrk 231 (Roche, Aitken & Whitmore 1983), two archetypal dusty Seyfert galaxies. PAH emission thus fails to appear even when the IR continuum is known to be largely thermal, implying that the PAHs must be missing.

2.3.2 What if the dusty clouds are optically thick?

Conceivably, radiative transfer effects within an irradiated, dusty cloud could suppress the contrast between the PAH features and the surrounding continuum, but such an arrangement would be highly unlikely. The near-UV photons that excite galactic PAH emission are absorbed by a typical dusty H I cloud within a column density $\lesssim 10^{21} \text{ cm}^{-2}$. Such a cloud becomes opaque to 3.3- μm radiation at $3 \times 10^{22} \text{ cm}^{-2}$ and to 11.3- μm radiation at $8 \times 10^{22} \text{ cm}^{-2}$ (Draine & Lee 1984), so the PAH emission is generated in what can be considered the cloud's chromosphere. Since the PAHs on the cloud's irradiated face will absorb about 40 per cent of the total UV power incident on grains (e.g. Puget & Léger 1989), the PAH re-emission will always be comparable to the UV-powered thermal continuum emission from larger grains. For the thermal continuum to overwhelm the PAH features, the larger grains would have to be selectively heated by a mechanism much more powerful than UV heating, but UV photons carry most of the power radiated by a typical AGN (e.g. Sanders et al. 1989) and are absorbed readily by dust grains.

Even in a contrived geometry in which we view only the back sides of thick, dusty clouds, it is still difficult to explain the absence of PAH emission without removing the PAHs themselves. The spectrum from the back side of a dusty, irradiated cloud will lack PAH features if the cloud is thicker than 10^{23} cm^{-2} , but the resulting thermal spectrum will be optically thick in the 9.7- μm silicate band. In such a thick cloud, absorption of the irradiating flux occurs inhomogeneously, with most of the energy deposited in a relatively thin layer at the irradiated face. The back side of this cloud will be substantially cooler than the front, creating a silicate absorption feature, which is seen only occasionally in AGN spectra (Roche et al. 1991). Thinner clouds ($10^{22-23} \text{ cm}^{-2}$) with intermediate mid-IR opacities would selectively extinguish the shorter wavelength features while transmitting the longer wavelength ones, and this effect is not observed.

3 PAH DESTRUCTION MODES

Energetic photons are thought to destroy PAHs in two basic ways: through photo-thermo dissociation (e.g. Léger et al. 1989) and through Coulomb explosion (Leach 1987). Photo-thermo dissociation is analogous to sublimation but relies on thermal transients rather than continuous equilibrium heating, while in Coulomb explosion the repulsive forces within a newly created, doubly charged PAH greatly reduce or eliminate the potential barrier to fragmentation. In practice, these processes are not entirely independent; simultaneous energy injection and lowering of the binding potential will reinforce one another. In this section, however, we will discuss them separately and then interpolate between measured PAH behaviour and solid-state grain behaviour to assess the stability of large PAHs, for which there are no laboratory measurements.

3.1 Photo-thermo dissociation

Clearly, if near-UV photons can heat PAHs to vibrational temperatures $\sim 1000 \text{ K}$, EUV photons and multiple-photon absorption events can potentially heat PAHs to several

thousand degrees, exceeding the equilibrium sublimation temperatures of even the most refractory substances. The probability of dissociation following superheating depends upon the size of the PAH, the precise amount of vibrational excitation (E_d), the time-scales for evaporation and radiative cooling, and the binding energies of the peripheral atoms (E_b). Detailed analyses of these various factors by Léger et al. (1989), Guhathakurta & Draine (1989) and others show that PAHs are remarkably resilient to evaporation, but that sufficiently large thermal transients, such as those induced by EUV photons, can be lethal.

Radiative dissociation of atoms from PAHs can be considered quasi-thermal because the electronic excitation of a PAH by a photon quickly (in $\sim 10^{-14} \text{ s}$) converts into vibrational excitation (Puget & Léger 1989; Allamandola et al. 1989). The work of Omont (1986) yields a convenient rule of thumb for evaluating the instantaneous energy input, E_d , needed to dissociate an atom of binding energy E_b from a PAH containing N_c carbon atoms: when $E_d \geq 0.1 E_b N_c$, a PAH will sublimate atoms more quickly than it can cool by emission of IR radiation. Thus PAHs with fewer than 20 or so carbon atoms will not survive stellar irradiation if $E_b \lesssim 7 \text{ eV}$.

Because H atoms bind less tightly to PAHs (4.8 eV) than to C atoms (8.5 eV) (Omont 1986), it has been thought that hydrogen will be shed before carbon upon superheating of a PAH (Omont 1986; Léger et al. 1989). Continual reaccretion of evaporated hydrogen could then buffer the carbon skeleton against dissociation. However, such arguments do not account for the sublimation of molecular fragments (Léger et al. 1989; Ruhl, Price & Leach 1989). Laboratory evaluations of PAH photodissociation show that C_2H_2 is the most easily removed species (Kim & Dunbar 1980), requiring significant carbon reaccretion to maintain the PAH against photodestruction. Section 4 will demonstrate how crucial the rate of carbon replacement is to the survival of PAHs near AGNs.

Recent laboratory studies of photon-PAH interactions have begun to quantify the damage done by EUV irradiation. Ruhl et al. (1989) find that photoionization of deuterated naphthalene (C_{10}D_8), a small PAH, by 20-eV photons yields $\text{C}_{10}\text{D}_7^+ + \text{D}$ (~ 30 per cent), $\text{C}_8\text{D}_6^+ + \text{C}_2\text{D}_2$ (~ 30 per cent), $\text{C}_6\text{D}_6^+ + \text{C}_4\text{D}_2$ (~ 20 per cent), and $\text{C}_{10}\text{D}_8^+$ (~ 20 per cent), and that C_2D_2 is bound to C_8D_6^+ by only 3.5 eV. As the incident photon energy increases through 40 eV, the fragmentation becomes more complete. Similar studies measuring the effects of X-rays on PAHs have not yet been performed, but X-ray destruction should be even more effective than UV destruction because thermalization of only a small fraction of the X-ray's energy will dissociate the molecule.

3.2 Coulomb explosion

Double ionization of PAH^0 to a PAH^{++} dication reduces both the covalent binding of the peripheral H atoms and the coherence of the carbon skeleton, often enabling additional excitation of the dication at the time of ionization to dissociate the PAH. Hydrogen removal is particularly easy: electron-impact experiments on anthracene ($\text{C}_{14}\text{H}_{10}$) show that ejection of two hydrogen atoms along with two electrons requires only a fraction of an eV more than double ionization

alone (Mathur et al. 1981). Removal of carbon-bearing fragments is not much harder: when doubly ionized by 40.8-eV photons, naphthalene will usually ‘Coulomb explode’ into two or more carbon-bearing pieces driven apart by internal electrostatic repulsion (Leach, Eland & Price 1989a).

The creation of unstable PAH dications can be either sequential, requiring photons of ≥ 7 eV for the first ionization and ≥ 13 eV for the second, or direct, with photons of ≥ 20 eV. Normally, Coulomb explosion of interstellar PAHs occurs only in H II regions because sequential ionization of PAHs by near-UV photons in H I clouds leaves the PAH dication with < 3 eV of internal energy, sufficient for hydrogen removal but not for more complete fragmentation (Leach 1987). However, X-rays can penetrate neutral media and doubly ionize PAHs both directly and through the Auger effect, rendering PAHs in active galaxies vulnerable, even in H I clouds.

Laboratory studies by Leach, Eland & Price (1989a, b) of naphthalene and some closely related compounds illustrate how the smaller PAHs behave following EUV photoionization. Generally, photons of $\lesssim 30$ eV create PAH^{++} less than 10 per cent of the time, and these dications tend not to Coulomb explode. As the ionizing photon energies rise to 40.8 eV, the PAH^{++} yield increases to 20 per cent, and the probability of Coulomb explosion becomes > 50 per cent. Beyond 40 eV, triple ionization will become important, and eventually, above the carbon *K*-edge at 284 eV, double ionization via the Auger process will dominate. Presumably, these high-energy events lead to Coulomb explosion with high probability.

3.3 X-ray destruction of larger PAHs

PAHs larger than naphthalene ($N_c = 10$) will behave more and more like solid-state graphitic planes as N_c rises. The photoelectric energy deposition into these larger systems will be two-fold. First, as in small PAHs, photoionization will leave the PAH in an excited electronic state that rapidly converts into an excited vibrational state. Then, as each photoelectron passes through the PAH and escapes, some of its kinetic energy will be degraded and thermalized into additional vibrational excitation. Since no detailed investigations studying the responses of large PAHs to X-radiation have yet been published, we will assess the stability of large PAHs under X-ray radiation by interpolating between the laboratory studies of small PAHs (Ruhl et al. 1989; Leach et al. 1989a, b), in which electronic excitation dominates, and solid-state models of small grain behaviour (Voit 1991), in which photoelectron degradation dominates.

Let us first consider the solid-state limit of photo-thermo dissociation. X-ray photoelectric absorption within a small graphite grain will eject one or more electrons which deposit ~ 4 eV \AA^{-1} each as they penetrate from the point of ionization to the grain’s surface and escape (Voit 1991). Since the diameter of a spherical graphite grain containing N_c carbon atoms is $\sim 3 N_c^{1/3}$ \AA , the maximum thermal energy an X-ray photoelectron can deposit is $E_{\text{max}} \sim 12 N_c^{1/3}$ eV. Using the rule of thumb from Section 3.1 and a C_2H_2 binding energy of 3.5 eV, we find that individual X-ray photoelectrons can photo-thermo dissociate C_2H_2 from spherical grains with $N_c \lesssim 200$. Simultaneous injection of an Auger electron along with the photoelectron can expel carbon from even larger

grains. Inasmuch as large PAHs retain similar amounts of an incident X-ray’s energy, they will be destroyed by X-radiation. Since PAHs are planar, however, the physics of photoelectron energy degradation within a PAH will differ somewhat.

In the molecular limit, photo-thermo dissociation begins with electronic excitation, so eventual expulsion of C_2H_2 from a large PAH requires an initial excitation $\sim 18 N_{50}$ eV, where $N_{50} = N_c/50$. Much of this excitation can result directly from X-ray photoionization. Photons more energetic than 284 eV will eject a carbon *K*-shell electron. Within 10^{-16} s Auger de-excitation will follow, filling the *K*-shell vacancy and ejecting a second electron. Auger electron spectroscopy of graphite shows that this process often induces 15–35 eV of valence-electron excitation (Houston & Rye 1988), sufficient to debind C_2H_2 from PAHs with $N_c \sim 50$ –100.

The processes that operate in these two limits are both capable of dissociating carbon-bearing fragments from larger PAHs. In addition, Coulomb repulsion within doubly ionized PAHs will reduce the binding of ionized fragments by $\sim N_{50}^{-1/2}$ eV. Throughout the remainder of this paper we will assume that carbon atoms are removed from large PAHs at a rate similar to the X-ray absorption rate. Although this assumption is plausible, more laboratory work is needed to prove that X-rays actually do expel carbon from PAHs with $N_c \sim 100$.

4 PAH DESTRUCTION/FORMATION BALANCE

The previous section showed that X-rays can expel carbonaceous fragments from PAHs; however, incremental destruction does not necessarily imply eradication. If the PAHs are to vanish, they must erode more quickly than they can rebuild. This section compares the rates at which atoms are ejected from and accreted on to PAHs in order to determine the conditions under which PAHs can survive in X-ray irradiated media.

4.1 Photodestruction rates

Only a few EUV/X-ray absorptions will completely destroy a small PAH and ~ 10 absorptions will vaporize a very small grain (Voit 1991), so the PAH photodestruction rate will be about an order of magnitude slower than the EUV/X-ray absorption rate. Fig. 1 shows the PAH photoionization cross-section per carbon atom measured by Verstraete et al. (1989). For comparison, the photoionization cross-section for atomic carbon given by the fits of Osterbrock (1989) and Voit (1991) are also shown. At 17–20 eV, the measured PAH cross-section per carbon atom exceeds the atomic carbon cross-section by a factor of 3, but above ~ 50 eV the PAH photoionization cross-section will be about equal to the sum of the cross-sections of its constituent atoms (Henke et al. 1982). Since the relevant photon energies are ≥ 200 eV (see Section 2.1) we use the fit of Voit (1991) to calculate the PAH photoabsorption rate.

The broad-band spectra of AGNs are adequately approximated by a power law with equal luminosity per logarithmic frequency interval. Here, we will parametrize the AGN radiance using the single parameter $L_0 = \nu L_\nu$, where L_ν is the

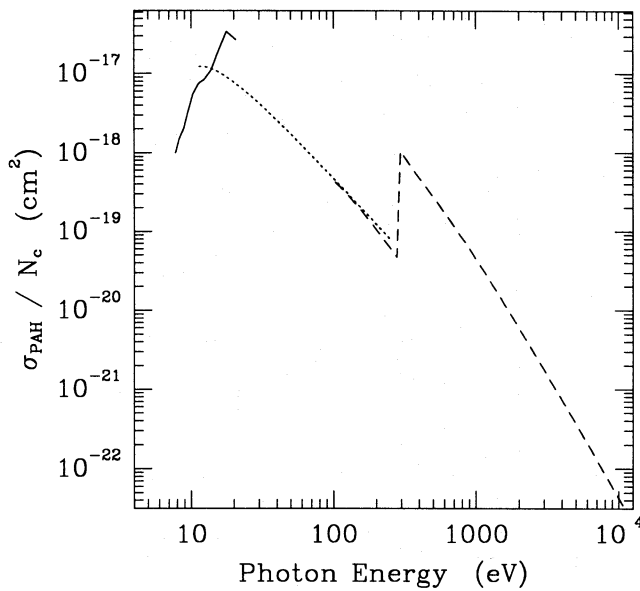


Figure 1. PAH cross-sections per carbon atom. The solid line gives the coronene ($\text{C}_{24}\text{H}_{12}$) cross-section per carbon atom measured by Verstraete et al. (1989). The dotted line illustrates the fit of Osterbrock (1989) to the atomic carbon photoionization cross-section, and the dashed line follows the fits of Voit (1991). Above 50 eV, the PAH cross-section should approach the sum of the cross-sections of its constituent atoms (Henke et al. 1982), so above the carbon K -edge at 284 eV the PAH cross-section per carbon atom is essentially equal to the cross-section of atomic carbon.

spectral luminosity of the AGN at frequency ν . Dim Seyferts have $L_0 \sim 10^{42}$ erg s^{-1} , brighter ones have $L_0 \sim 10^{44}$ erg s^{-1} , and quasars have $L_0 \sim 10^{46}$ erg s^{-1} . In actual AGN spectra, L_0 drops by a factor of several from the UV into the X-ray band (e.g. Sanders et al. 1989), but since X-ray shielding is very important to PAH survival (see Section 5.1), the relevant value of L_0 can be evaluated at the wavelength where the optical depth of the shielding layer is roughly unity.

Fig. 2 shows the X-ray photoabsorption rates for PAHs of 50 carbon atoms at a distance of 1 kpc from an $L_0 = 10^{44}$ erg s^{-1} AGN shrouded by various column densities of neutral absorbing gas. The opacity of the absorbing gas, assumed to have cosmic abundances, is taken from Morrison & McCammon (1983). A shielding column density of greater than 10^{23} cm^{-2} is necessary if the PAHs are to live a significant length of time ($> 10^4$ yr) in this ISM. The PAH destruction rate will vary linearly with the photon flux and will increase weakly as the PAH becomes smaller. We discuss X-ray shielding in more detail in Section 5.1.

4.2 Accretion rates

The importance of PAHs to the chemistry of the interstellar medium has been discussed by several authors (e.g. Omont 1986; Lepp & Dalgarno 1988), but here we are more concerned with how the interstellar medium affects the constitution of PAHs. Atoms and ions of hydrogen and carbon, as they pass through the ISM, will encounter PAHs and occasionally stick to them, adding to their bulk. The precise chemistry of these reactions is unknown, but rough

estimates of hydrogen and carbon accretion will allow us to determine the fate of PAHs near AGNs.

According to Omont (1986), a PAH containing N_c carbon atoms has a surface area $\sim 2.5 N_c \text{ \AA}^2$ and a polarizability of $10^{-24} N_c^{3/2} \text{ cm}^3$, neutral atoms have a polarizability of 10^{-24} cm^3 , and about one-third of the atoms that encounter the surface of a PAH will stick. So, in an H I cloud of temperature T_2 (100 K), the geometrical rate coefficient for accretion of H^0 on to PAH^0 is

$$R_{\text{H}^0, \text{geo}} \sim (6 \times 10^{-10} \text{ cm}^3 \text{ s}^{-1}) \frac{Y}{0.3} N_{50} T_2^{1/2}, \quad (1)$$

where Y is the effective sticking coefficient. Polarization interactions between PAH^+ and H^0 induce additional accretion of hydrogen with a rate coefficient

$$R_{\text{H}^0, \text{pol}} \sim (7 \times 10^{-10} \text{ cm}^3 \text{ s}^{-1}) \frac{Y}{0.3}. \quad (2)$$

The analogous rate coefficients for accretion of neutral carbon are smaller by a factor of $\sqrt{12}$, but since the near-UV photons within an H I cloud ionize most of the C^0 to C^+ , polarization interactions between PAH^0 and C^+ , with a rate coefficient

$$R_{\text{C}^+, \text{pol}} \sim (4 \times 10^{-9} \text{ cm}^3 \text{ s}^{-1}) \frac{Y}{0.3} N_{50}^{3/2}, \quad (3)$$

will dominate the carbon accretion. At temperatures $\sim 10^4$ K and lower, Coulomb repulsion prohibits accretion of C^+ on to PAH^+ . Permanent binding of an accreted atom will depend upon its proximity to a radical site at the periphery of the PAH. In the most quiescent regions of the ISM, peripheral radical sites might be rare, but in X-ray irradiated clouds they ought to be common.

Because ionization balance enters into the carbon accretion rate, PAH survival will be determined, in part, by the ambient near-UV flux and the local electron density. The ratio of the PAH^+ and PAH^0 number densities found by Omont (1986) is

$$\frac{n_{\text{PAH}^+}}{n_{\text{PAH}^0}} \sim 10^{-4} \frac{\chi}{\chi_{\text{ISM}}} \frac{Y}{0.3} P_{12}^{-1} N_{50}^{1/2} T_2^{3/2} f_e^{-1}, \quad (4)$$

where χ is the ambient near-UV photon intensity, $\chi_{\text{ISM}} \sim 10^7$ photon $\text{cm}^{-2} \text{ s}^{-1} \text{ sr}^{-1}$ is the near-UV photon intensity in the solar neighbourhood, P_{12} is the cloud pressure in units of 10^{12} erg cm^{-3} , f_e is the free-electron abundance relative to hydrogen, and we have taken the PAH photoionization cross-section to be $\sim 10^{-17} \text{ cm}^2$ in the near-UV. The fraction $f_{\text{PAH}^0} = (1 + n_{\text{PAH}^+}/n_{\text{PAH}^0})^{-1}$ is of order unity in a typical H I cloud, where $f_e > 5 \times 10^{-4}$ and $\chi \sim 1$; however, when χ rises by more than an order of magnitude, f_{PAH^0} can begin to drop below unity, inhibiting C accretion and impairing the ability of PAHs to repair themselves. This could be why the PAH abundance in the Galactic ISM appears to drop when the ambient radiation field exceeds that in the solar neighbourhood by a factor ≥ 16 (Boulanger et al. 1988).

In Fig. 2 we plot the carbon and hydrogen accretion time-scales (per PAH) derived from these rate coefficients, to facilitate comparison with the X-ray photoabsorption time-

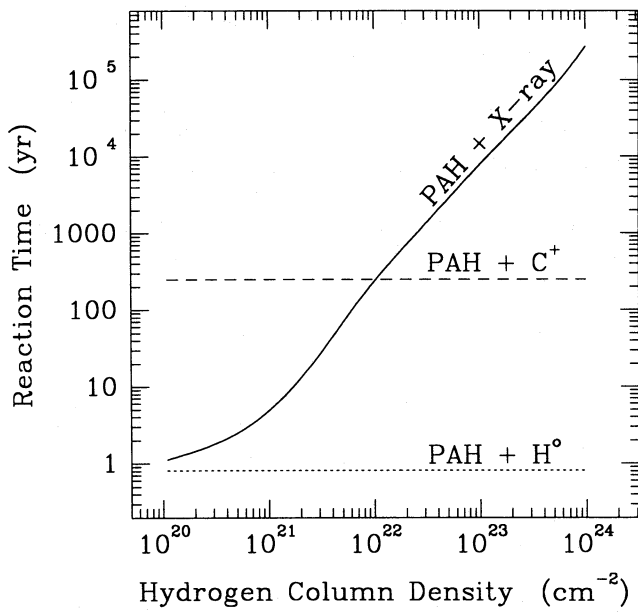


Figure 2. Reaction times for the accretion and ejection of hydrogen and carbon. The solid line gives the time-scale for X-ray photoionization of a PAH ($N_c = 50$) at 1 kpc from an $L_0 = 10^{44}$ erg s $^{-1}$ AGN shielded by solar-abundance clouds having neutral hydrogen column densities of 10^{20} to 10^{24} cm $^{-2}$. The dotted line gives the approximate hydrogen accretion time-scales, through both polarization and geometrical interactions, on to a PAH ($N_c = 50$, $Y = 0.3$) in an ISM cloud where $P_{12} = T_2 = 1$, and the dashed line gives the carbon accretion time-scale for $P_{12} = T_2 = f_{\text{PAH}^0} = 1$. For a given column density, the photoionization time, which will be of order the carbon ejection time-scale, varies inversely with the photon flux and weakly with N_c . The geometrical hydrogen accretion time varies as $Y^{-1} N_{50}^{-1} P_{12}^{-1} T_2^{1/2}$, and the polarization accretion time varies as $Y^{-1} P_{12}^{-1} T_2$. The carbon accretion time varies as $Y^{-1} N_{50}^{-3/2} P_{12}^{-1} T_2 f_{\text{PAH}^0}$.

scales. We assume $P_{12} = T_2 = 1$ (implying a hydrogen density $n_{\text{H}} = 65$ cm $^{-3}$), $N_{50} = 1$, $f_{\text{PAH}^0} = 1$, and an abundance of carbon relative to hydrogen of 4.9×10^{-4} (Grevesse 1984). The actual accretion time-scales are proportional to $P_{12}^{-1} T_2$, via the density factor, and the time-scale for carbon accretion is also proportional to $f_{\text{PAH}^0}^{-1}$. Even when carbon is accreting at the maximum rate ($f_{\text{PAH}^0} \sim 1$), a shielding hydrogen column density $\lesssim 10^{22}$ cm $^{-2}$ is needed to preserve PAHs at 1 kpc from an $L_0 \sim 10^{44}$ erg s $^{-1}$ AGN. Moreover, the near-UV radiation at this distance from the AGN, of order $400 \chi_{\text{ISM}}$, can suppress the C accretion rate by reducing f_{PAH^0} , thereby increasing the shielding requirement.

4.3 PAH survival and ionization parameter

The survival of PAHs is analogous to the persistence of neutral atoms in an ionizing radiation field and can be related to the ionization parameter $U = n_{\text{ph}}/n_{\text{H}}$, where n_{ph} is the number density of ionizing photons. At a column depth $\sim 10^{20}$ cm $^{-2}$ within an H I cloud, the PAH fragmentation rate will be closely related to the carbon K-shell photoionization rate. Assuming νL_{ν} is constant throughout the ionizing spectrum, the K-shell ionization and C $^{+}$ accretion rates will

be equal at the critical ionization parameter

$$U_{\text{C}}^{\text{cr}} \sim 10^{-4} f_{\text{PAH}^0} \frac{Y}{0.3} N_{50}^{1/2}. \quad (5)$$

Hence, at ionization parameters $\log U \sim -2$ to -2.5 , typical of emission-line clouds in AGNs, PAHs will not survive. Only at radii greater than

$$r_{\text{C}}^{\text{cr}} \sim (14 \text{ kpc}) \times \left(\frac{L_0}{10^{44} \text{ erg s}^{-1}} \right)^{1/2} \left(\frac{Y}{0.3} \right)^{-1/2} P_{12}^{-1/2} T_2^{1/2} f_{\text{PAH}^0}^{-1/2} N_{50}^{-1/4} \quad (6)$$

will carbon reaccretion dominate K-shell photoionization. Why, then, do PAH features sometimes appear in AGN spectra, if PAHs are so easily destroyed?

5 PAH SURVIVAL IN ACTIVE GALAXIES

Although PAH features usually do not appear in the mid-IR spectra of active galaxies, they are present in a few cases (Désert & Dennefeld 1988; Roche et al. 1991). The PAH emission from one such galaxy (NGC 7469) is clearly extended (Cutri et al. 1984) and is associated with a circumnuclear starburst. Section 4 argues that PAHs this close to an AGN (< 1 kpc) ought to be destroyed by the intense X-radiation. Here we will show that PAHs can survive if they are shielded from the AGN's X-ray emission by a large column density of X-ray absorbing material, and we will discuss how PAH emission mapping can be used to study the propagation of X-radiation in active galaxies.

5.1 The importance of shielding

The results of Section 4, presented in Fig. 2, show that PAH survival within a few kiloparsecs of a typical Seyfert nucleus is extremely unlikely if the PAH is exposed to the full flux emanating from the AGN. Reaccretion of carbon will be fast enough only for ISM pressures several orders of magnitude greater than that in the solar neighbourhood. A more likely possibility is that the AGN flux towards the PAH is obscured by intervening material.

A hydrogen column density N_{H} of neutral gas lying between an AGN and a PAH transmits photons of $\geq (1 \text{ keV}) [N_{\text{H}} / (4 \times 10^{21} \text{ cm}^{-2})]^{0.4}$ and blocks lower energy photons (Morrison & McCammon 1983). Since the K-shell absorption cross-section of a PAH drops like the inverse cube of the photon energy, the X-ray absorption time for a PAH irradiated by a constant νL_{ν} power-law spectrum will vary as $N_{\text{H}}^{1.6}$. Fig. 2 shows how the X-ray absorption time rises as the obscuring column density increases.

Attenuation of the AGN spectrum also changes the critical ionization parameter, so that

$$U_{\text{C}}^{\text{cr}}(N_{\text{H}}) \sim (5 \times 10^{-9}) \frac{Y}{0.3} N_{50}^{1/2} f_{\text{PAH}^0} \frac{1}{\Sigma(N_{\text{H}})}, \quad (7)$$

where

$$\Sigma(N_{\text{H}}) = \frac{1}{\sigma_{\text{g}}} \frac{\int F_{\text{ph}}(E, N_{\text{H}}) \sigma_{\text{d}}(E) dE}{\int F_{\text{ph}}(E, N_{\text{H}}) dE}. \quad (8)$$

Here, E is the photon energy, $F_{\text{ph}}(E, N_{\text{H}})$ is the spectral photon flux incident on the cloud after it has passed through an absorbing column N_{H} , $\sigma_{\text{d}}(E)$ is the cross-section for photodissociation of carbon from a PAH, and σ_{g} is the geometrical cross-section of the PAH. Fig. 3 illustrates $[\Sigma(N_{\text{H}})]^{-1}$ for a constant νL_{ν} spectrum when $\sigma_{\text{d}}(E)$ is taken to be the K -shell photoionization cross-section.

X-ray observations of NGC 7469 support the X-ray shielding hypothesis. The *Ginga* X-ray spectrum of this galaxy contains a hard X-ray reflection component (Piro, Yamauchi & Matsuoka 1990), which indicates the presence of thick ($> 10^{24} \text{ cm}^{-2}$), cool ($< 10^6 \text{ K}$) obscuring gas near the active nucleus (Lightman & White 1988; George & Fabian 1991). The X-ray flux along the unobscured line of sight from this AGN towards the Earth converts to an isotropic X-ray luminosity of $\sim 3 \times 10^{43} \text{ erg s}^{-1}$. PAHs in the starburst ring at $< 1 \text{ kpc}$ from this AGN cannot withstand unobscured X-ray irradiation at this level, so the escape of X-radiation must be anisotropic, with PAHs surviving only in the shadows cast by obscuring material nearer the active nucleus.

5.2 AGN anisotropy and PAH mapping

As emission-line images of the matter immediately surrounding AGNs have become more detailed, elongated extended emission-line regions have become evident (e.g. Pogge 1988, 1989; Evans et al. 1991). These nebulae, often having

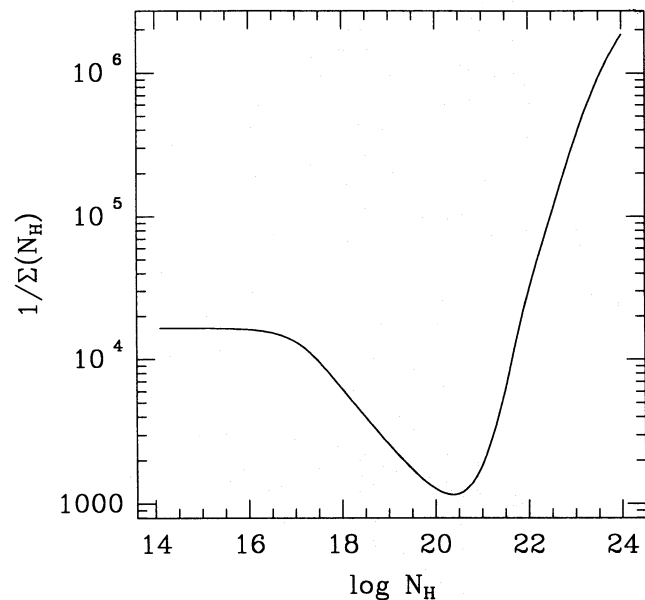


Figure 3. Σ^{-1} as a function of shielding column density N_{H} . The function Σ is the dimensionless cross-section for photodissociation of carbon from a PAH, weighted by the photon energy spectrum. Here we assume that only K -shell photoionizations lead to dissociation and show Σ^{-1} for a constant νL_{ν} AGN spectrum attenuated by an intervening column N_{H} (in cm^{-2}) of neutral absorbing gas. As $\log N_{\text{H}}$ rises from 17 to 20, EUV photons are absorbed by the shielding cloud, but soft X-ray photons are not, so Σ^{-1} drops. Above $\log N_{\text{H}} \approx 20.5$ the intervening material shields PAH-destroying soft X-ray photons more effectively, so Σ^{-1} rises, and PAHs can survive at higher ionization parameters.

position angles similar to radio jets (McCarthy et al. 1987), are thought to occur either because the radiation from the AGN is beamed along the axis of elongation, or because the ionizing radiation perpendicular to this axis has been obscured, perhaps by a torus of molecular gas. Above, we have shown that PAHs survive near AGNs only when they cannot see the X-ray flux from the central engine; thus, PAHs offer a way to see where ionizing radiation is absent, complementing the emission-line maps that show us where ionizing radiation is present. Two-dimensional PAH mapping can uniquely probe the angular distribution of X-ray obscuration in an active galaxy, but PAH emission will be observable only if the PAHs are illuminated by a sufficient number of bright stars and will trace only those regions of starburst activity that are not subject to X-ray irradiation.

5.3 Distinguishing AGNs from normal starbursts

The presence or absence of PAH emission in the mid-IR discriminates strongly between starburst galaxies and AGNs. The preceding discussions demonstrate that PAHs are selectively destroyed by X-rays, so that, in a more general sense, the presence of PAH emission indicates a soft (UV) radiation field, whereas its absence signals a hard (EUV/X-ray) radiation field. In the occasional cases where PAH features are observed in active galaxies, they cannot be excited directly by the AGN and must therefore be emerging from shielded starburst regions. The following guidelines prescribe how PAH emission can be used as an AGN/starburst diagnostic: (i) luminous galactic nuclei with featureless mid-IR continua are either non-thermal IR emitters or they contain a source of hard ionizing radiation likely to be an AGN, (ii) in galactic nuclei with prominent PAH emission, stars must contribute a large fraction of the total luminosity because AGN-irradiated clouds emit no PAH features, and (iii) in some galaxies containing both an active nucleus and a circumnuclear starburst of comparable luminosity (e.g. NGC 7469), the relative importance of the PAH emission, determined by the shielding of the AGN, gives a lower limit to the energetic importance of the starburst.

6 CONCLUSIONS

Mid-IR spectra of starburst and Seyfert galaxies differ strikingly; starburst galaxies emit prominent PAH features, while Seyfert galaxies usually do not. Even some dusty Seyfert galaxies show no PAH features, indicating that PAHs have somehow been selectively removed from their inner regions. Penetrating X-rays, much more common in active galaxies than in starbursts, can accomplish this selective eradication.

Small PAHs, containing ~ 10 carbon atoms, have been shown to fragment thoroughly after absorption of an EUV photon, and will be destroyed rapidly by X-rays. Theoretical arguments suggest that carbon K -shell photoionization can eject carbon-bearing fragments from PAHs up to 200 carbon atoms in size, but laboratory experiments are needed to determine how large a PAH must be before it can withstand X-ray irradiation without evaporating. PAHs below this threshold will shed carbon atoms at roughly the K -shell photoionization rate and will not survive unshielded in the ISM within a kiloparsec of even a weak AGN.

Nevertheless, ~ 10 per cent of Seyfert galaxies show some PAH emission. The emitting PAHs within these galaxies presumably exist in circumnuclear starburst regions shielded from the AGN by a large column density of X-ray absorbing gas. Narrow-band 3.3- μm imaging of these objects should then reveal the directions within the host galaxy along which the AGN radiation has been obscured, complementing optical forbidden-line maps that show where the AGN radiation has escaped. In addition, PAH mapping, because it distinguishes starburst from Seyfert activity, should provide insights into possible AGN–starburst connections, particularly in hybrid galaxies like NGC 7469 where both phenomena are energetically important.

ACKNOWLEDGMENTS

The author would like to thank S. Phinney, M. Shull and T. Soifer for enlightening conversations, and acknowledges the support of NASA Grants NAGW-2142 and NAGW-2144.

REFERENCES

- Aitken D. K., Roche P. F., 1985, *MNRAS*, 213, 777
 Allamandola L. J., Tielens A. G. G. M., Barker J. R., 1985, *ApJ*, 290, L25
 Allamandola L. J., Tielens A. G. G. M., Barker J. R., 1989, *ApJS*, 71, 733
 Boulanger F., Beichman C., Desert F. X., Helou G., Perault M., Ryter C., 1988, *ApJ*, 332, 328
 Carleton N. P., Elvis M., Fabbiano G., Willner S. P., Lawrence A., Ward M., 1987, *ApJ*, 318, 595
 Cutri R. M., Rudy R. J., Rieke G. H., Tokunaga A. T., Willner S. P., 1984, *ApJ*, 280, 521
 Désert F. X., Dennefeld M., 1988, *A&A*, 206, 227
 Donn B. D., Allen J. E., Khanna R. K., 1989, in Allamandola L. J., Tielens A. G. G. M., eds, *Interstellar Dust*. Kluwer, Dordrecht, p. 181
 Draine B. T., Lee H. M., 1984, *ApJ*, 285, 89
 Evans I. N., Ford H. C., Kinney A. L., Antonucci R. R. J., Armus L., Caganoff S., 1991, *ApJ*, 369, L27
 George I. M., Fabian A. C., 1991, *MNRAS*, 249, 352
 Giard M., Pajot F., Lamarre J. M., Serra G., Caux E., Gispert R., Léger A., Rouan D., 1988, *A&A*, 201, L1
 Grevesse N., 1984, *Phys. Scripta*, T8, 49
 Guhathakurta P., Draine B. T., 1989, *ApJ*, 345, 230
 Henke B. L., Lee P., Tanaka T. J., Shimabukuro R. L., Fujikawa B. K., 1982, *Atom. Data Nucl. Tables*, 27, 1
 Houston J. E., Rye R. R., 1988, in Briant C. L., Messmer R. P., eds, *Auger Electron Spectroscopy*. Academic Press, Boston, p. 65
 Kim M. S., Dunbar R. C., 1980, *J. chem. Phys.*, 72, 4405
 Leach S., 1987, *J. Electr. Spectrosc.*, 41, 427
 Leach S., Eland J. H. D., Price S. D., 1989a, *J. Phys. Chem.*, 93, 7575
 Leach S., Eland J. H. D., Price S. D., 1989b, *J. Phys. Chem.*, 93, 7583
 Leger A., Puget J. L., 1984, *A&A*, 137, L5
 Léger A., Boissel P., Désert F. X., d'Hendecourt L., 1989, *A&A*, 213, 351
 Lepp S., Dalgarno A., 1988, *ApJ*, 324, 553
 Lightman A. P., White T. R., 1988, *ApJ*, 335, 57
 Mathur B. P., Burgess E. M., Bostwick D. E., Moran T. F., 1981, *Org. Mass Spectrosc.*, 16, 92
 McCarthy P. J., van Breugel W. J. M., Spinrad H., Djorgovski S. G., 1987, *ApJ*, 321, L29
 Moorwood A. F. M., 1986, *A&A*, 166, 4
 Morrison R., McCammon D., 1983, *ApJ*, 270, 119
 Omont A., 1986, *A&A*, 164, 159
 Osterbrock D. E., 1989, *Astrophysics of Gaseous Nebulae and Active Galactic Nuclei*. University Science Books, Mill Valley, CA
 Piro L., Yamauchi M., Matsuoka M., 1990, *ApJ*, 360, L35
 Pogge R. W., 1988, *ApJ*, 328, 519
 Pogge R. W., 1989, *ApJ*, 345, 730
 Puget J. L., Léger A., 1989, *ARA&A*, 27, 161
 Roche P. F., Aitken D. K., Whitmore B., 1983, *MNRAS*, 205, 21P
 Roche P. F., Aitken D. K., Phillips M. M., Whitmore B., 1984, *MNRAS*, 207, 35
 Roche P. F., Aitken D. K., Smith C. H., Ward M. J., 1991, *MNRAS*, 248, 606
 Ruhl E., Price S. D., Leach S., 1989, *J. Phys. Chem.*, 93, 6312
 Sanders D. B., Phinney E. S., Neugebauer G., Soifer B. T., Matthews K., 1989, *ApJ*, 347, 29
 Sellgren K., 1981, *ApJ*, 245, 138
 Sellgren K., 1984, *ApJ*, 277, 623
 Verstraete L., Léger A., d'Hendecourt L., Dutuit O., Défourneau D., 1989, in Tielens A. G. G. M., Allamandola L. J., eds, *Interstellar Dust: Contributed papers*. NASA CP-3036, Washington DC, p. 183
 Voit G. M., 1991, *ApJ*, 379, 122